

Article

The Repurposing of the Antimalaria Drug, Primaquine, as a Photosensitizer to Inactivate Cryptococcal Cells

Uju L. Madu, Adepemi O. Ogundeji , Olufemi S. Folorunso , Jacobus Albertyn, Carolina H. Pohl 
and Olihile M. Sebolai * 

Department of Microbiology and Biochemistry, University of the Free State, 205 Nelson Mandela Drive, Park West, Bloemfontein 9301, South Africa; lynda.madu@yahoo.com (U.L.M.); ogundejiao@ufs.ac.za (A.O.O.); foxyphemzy@gmail.com (O.S.F.); albertynj@ufs.ac.za (J.A.); pohlch@ufs.ac.za (C.H.P.)

* Correspondence: sebolaiom@ufs.ac.za; Tel.: +27-51-401-2004

Abstract: Cryptococcal cells can manifest skin infections in immunocompromised persons. While it may be easy to diagnose cryptococcal infection, treatment often fails due to the ineffectiveness of current antifungal agents. To this end, the present study explored the repurposing of primaquine (PQ), as a photosensitizer. PDT was carried out using a germicidal ultraviolet (UV) lamp, which has a radiation output of approximately $625 \mu\text{W}/\text{cm}^2$ at a distance of 20 cm. When compared to the non-treated cells, the metabolic activity of cryptococcal cells was significantly ($p < 0.05$) limited. The photolytic products of PQ were observed to alter the ultrastructure of treated cells. The latter was not incidental, as the same cells were also documented to lose their selective permeability. Importantly, PDT also improved the efficiency of macrophages to kill internalized cryptococcal cells ($p \leq 0.05$) when compared to non-treated macrophages. Equally importantly, PDT was not detrimental to macrophages, as their metabolic activity was not significantly ($p > 0.05$) limited, even when exposed to $20\times$ the MIC (determined for cryptococcal cells) and an exposure time that was $4\times$ longer. Taken together, the results suggest PQ has the potential to control the growth of cryptococcal cells and limit their survival inside the macrophage.

Keywords: *Cryptococcus*; inactivation; macrophages; photodynamic therapy; photosensitizer; Primaquine (PQ); Ultraviolet Light (UV)



Citation: Madu, U.L.; Ogundeji, A.O.; Folorunso, O.S.; Albertyn, J.; Pohl, C.H.; Sebolai, O.M. The Repurposing of the Antimalaria Drug, Primaquine, as a Photosensitizer to Inactivate Cryptococcal Cells. *Photochem* **2021**, *1*, 275–286. <https://doi.org/10.3390/photochem1020017>

Academic Editor: Anna Clea Croce

Received: 31 July 2021

Accepted: 29 August 2021

Published: 7 September 2021

Publisher's Note: MDPI stays neutral with regard to jurisdictional claims in published maps and institutional affiliations.



Copyright: © 2021 by the authors. Licensee MDPI, Basel, Switzerland. This article is an open access article distributed under the terms and conditions of the Creative Commons Attribution (CC BY) license (<https://creativecommons.org/licenses/by/4.0/>).

1. Introduction

The skin is home to complex microbial communities, reflecting the biodiversity of the ecosystems they inhabit [1]. Importantly, the skin also provides the first line of protection against pathogens [2], for example, by the tactical arrangement of dendritic cells (CD103⁺) for the cross-presentation of skin-tropic pathogens [3].

Presentation of a portal of entry, i.e., a mechanical injury to the skin due to insertion of a medical device, can create an opportunity for commensal organisms to invade a host. In this regard, the chances of direct inoculation are also increased. *Cryptococcus (C.) neoformans* is an example of an airborne environmental fungus that can cause a primary skin infection following direct inoculation—although such instances are rare [4,5]. In the main, following a primary lung infection in a person with a weakened immune system, cells could disseminate “freely” in the blood or hide inside invaded macrophages in a Trojan horse-like manner [6,7]. Such cells can practically reach every organ system of the body [6,7], including the skin [4].

Rajasingham et al. documented that sub-Saharan Africa has the highest cryptococcal meningitis mortality rate in the world, i.e., 75% of all recorded cases [8]. This high mortality rate is in part due to the limited number of available antifungals [9]. The current treatment regimen is limited to amphotericin B, fluconazole, and flucytosine. However, flucytosine, which is more effective against cryptococcal infections, is less frequently used in resource-limited settings due to cost implications. Amphotericin B and fluconazole are

generally used in South Africa [10], and their mechanism of action targets the fungal cell membrane [11]. Unfortunately, therapy with these two drugs has contributed to unacceptably high mortality rates due to clinical failure [12]. Additionally, amphotericin B has been associated with considerable nephrotoxicity and poor ability to penetrate the blood–brain barrier due to its chemical and physical nature [13–15]. Conversely, fluconazole has been reported to be associated with poorer clinical outcomes due to clinical relapse and the risk of inducing drug resistance [16–18]. It is, therefore, crucial to explore alternative therapy to combat antifungal host toxicity and resistance, as the evolution of this resistance is outpacing the current antifungal agents. Several treatment options have been reconsidered in the quest for alternative treatment.

The current study considers photodynamic treatment (PDT) as a possible solution to control primary cutaneous cryptococcosis (PCC). PDT has, for some time, been a well-studied therapeutic option that involves the optimal combination of a light-sensitive compound (photosensitizer) and light of a specific absorption wavelength in the presence of ambient air [19,20]. The treatment induces the accumulation of harmful radicals that fix on cellular components of a targeted organism leading to cell death [19–23]. An ideal photosensitizer is a chemical compound with suitable photo-physical characteristics that can induce a specific photo-activity effect [24]. To this end, a few compounds have been proven to be ideal photosensitizers when applied against several microbes [25]. A well-known photosensitizer is phenothiazinium salt (methylene blue), which has been shown to inactivate the growth of bacteria, fungi, and protozoa [26].

In this study, PQ is repurposed as a photosensitizer that may inactivate the highly aerobic cryptococcal cells. Traditionally, PQ is widely used in malaria therapy, and it is thought to disrupt the mitochondrial function of the aerobic *Plasmodium* [27–30]. Notably, the idea of repurposing PQ is not foreign, as it has successfully been shown to control the growth of *Pneumocystis jirovecii* [31,32]. It is, therefore, theorized that PDT would be successful when used against aerobic microbes, similarly to *Plasmodium* and *Pneumocystis jirovecii*, given their natural susceptibility to oxidative damage [19,33].

2. Materials and Methods

2.1. Materials

Yeast extract, malt extract, peptone, glucose, agar (Merck, Johannesburg, South Africa), phosphate buffer solution (PBS) (Sigma-Aldrich, Johannesburg, South Africa), RPMI-1640 medium, fetal bovine serum (Biochrom, Berlin, Germany), penicillin, streptomycin (Sigma-Aldrich, St. Louis, MO, USA), l-glutamine (Sigma-Aldrich, Johannesburg, South Africa), trypan blue stain, 0.1% Triton X-100 (Sigma-Aldrich, South Africa), hemocytometer (Marienfeld, Germany), sterile disposable 96-well flat-bottom microtiter plate (Greiner Bio-One, Frickenhausen, Germany), absolute ethanol (Merck, South Africa), propidium iodide (PI) (Life Technologies, Carlsbad, CA, USA), Toxilight (Lonza Rockland, Inc., Rockland, ME, USA), sodium-phosphate-buffered 3% glutardialdehyde (Merck, Johannesburg, South Africa), sodium-phosphate-buffered 3% osmium tetroxide (Merck, Johannesburg, South Africa), 5, 2',7-dichlorofluorescein diacetate (DCFHDA) (Sigma-Aldrich, Johannesburg, South Africa), 2,3-bis (2-methoxy-4-nitro-5-sulfophenyl)-5-[(phenylamino)carbonyl]-2H-tetrazolium hydroxide (XTT; Sigma-Aldrich, Johannesburg, South Africa), menadione (Sigma-Aldrich, Johannesburg, South Africa), 1.5 mL plastic tubes (Merck, South Africa), germicidal ultraviolet light (UVL) lamp (ESCO, Johannesburg, South Africa), Airstream[®] Class II Biological Safety Cabinet (ESCO, Johannesburg, South Africa), SEM coating system (Bio-Rad Microscience Division, Johannesburg, South Africa), Shimadzu Super-scan SSX 550 SEM (Shimadzu, Tokyo, Japan), spectrophotometer (EZ Read 800 Research; Biochrom, United Kingdom), and Fluoroskan Ascent FL microplate reader (Thermo Scientific, Waltham, MA, USA).

2.2. Cells, Cultivation and Standardization

The prototypical cryptococcal reference strain, i.e., *C. neoformans* H99, was used in the study. This organism was streaked out on fresh, sterile, yeast-malt-extract (YM) agar (3 g/L yeast extract, 3 g/L malt extract, 5 g/L peptone, 10 g/L glucose, 16 g/L agar). The plates were incubated for 48 h at 30 °C. After 48 h, a single colony was scooped with an inoculation loop and streaked onto a fresh, sterile YM agar plate before incubating for 24 h at 30 °C. After the incubation period, five colonies were suspended in 5 mL of sterile distilled water. A McFarland standard of 0.5 was prepared to obtain a cell concentration between 0.5×10^5 and 2.5×10^5 colony forming units (CFU) per mL.

A murine macrophage cell line, RAW 264.7 (TIB-71 from ATCC), was cultivated in a tissue flask containing 10 mL of RPMI-1640 medium. The medium was supplemented with 20 mg/mL streptomycin, 2 mM L-glutamine, 20 U/mL penicillin and 10% fetal bovine serum. The flask was incubated at 30 °C in a 5% CO₂ incubator until confluence was reached. The cells were harvested, and their viability was determined to be 90% after staining with trypan blue. Thereafter, the cell concentration of macrophages was determined using a hemocytometer. The cell concentration was adjusted to a final cell concentration of 1×10^6 cells/mL using a 10 mL solution of fresh, sterile RPMI-1640 medium. A 100 µL suspension of cells was then dispensed into wells of a sterile 96-well flat-bottom microtiter plate. The plate was incubated overnight in 5% CO₂ at 37 °C. Before use, the overnight spent media was aspirated and replaced with 100 µL of fresh, sterile RPMI-1640 media.

2.3. UV Radiation

Photosensitizer: PQ was obtained from Sigma-Aldrich as a standard powder. The PQ stock solution was prepared in distilled water to yield a stock solution of 1200 µM. The drug was further diluted in RPMI-1640 medium to reach final concentrations of 0, 6, 15, 30, 60, and 600 µM. The final amount of distilled water in RPMI-1640 media never exceeded 1%. The UV/Vis absorption of PQ was determined to be 260 nm (data not shown), which was in the UVC range of the germicidal lamp.

Light source: A germicidal ultraviolet C (UVC) lamp that was fitted in a Class II Biological safety cabinet (ESCO, South Africa) was used as the light source. The lamp is reported to have a nominal power of 30 watts. In the current study, the cells were kept at a distance of approximately 20 cm from the lamp. At this distance, the lamp is estimated to have a radiation output of 625 µW/cm² [34].

2.4. Preparation of Cells for Experimental Assays

A 100 µL standardized inoculum of cryptococcal cells (0.5×10^5 and 2.5×10^5 CFU/mL) was dispensed into wells of sterile 96-well flat-bottom microtiter plates. To the same wells, 100 µL of the prepared compounds were added. A number of experimental conditions were set up at room temperature to assess the effect of PDT using PQ on cryptococcal cells. These were: (1) cryptococcal cells with 0 µM of PQ and exposed to dark light (DL) for 2 min (i.e., non-treated (non-Rx) cells); (2) cryptococcal cells with 6 µM, 30 µM or 60 µM of PQ and exposed to DL for 2 min (i.e., drug effect); (3) cryptococcal cells with 0 µM of PQ and exposed to ultraviolet light (UVL) for 2 min (i.e., UV effect), and (4) cryptococcal cells with 6 µM, 30 µM or 60 µM of PQ and exposed to UVL for 2 min (i.e., PDT effect). The cells were first allowed to react to PQ for 30 min (in the dark) prior to exposure to UVL (where appropriate).

2.5. Metabolic Activity Assay of Cryptococcal Cells

Following the handling of cryptococcal cells per the above conditions, they were reacted with a tetrazolium salt (2,3-bis-(2-methoxy-4-nitro-5-sulfophenyl)-2H-tetrazolium-5-carboxanilide, XTT) and menadione. This reaction produces a soluble formazan salt.

The plates were incubated for 3 h at 37 °C in 5% CO₂. After 3 h of initiating the tetrazolium reaction, the absorbance of the wells was measured at 492 nm. The amount of formazan formed is directly related to the metabolic activity of cells.

2.6. Effects of PDT with PQ on the Accumulation of Reactive Oxygen Species (ROS)

The levels of accumulated ROS were measured using 2',7-dichlorofluorescein diacetate (DCFHDA). In brief, following the treatment of cells as indicated in the in vitro susceptibility assay section, the micro-well contents were aspirated and dispensed to corresponding wells in a black microtiter plate. Thereafter, 10 µL of DCFHDA (1 mg/mL) was reacted with 90 µL of the aspirated cells suspension. The plates were incubated at room temperature for 30 min in the dark. Induced fluorescence was measured at excitation and emission of 485/535 nm using a fluorescence plate reader.

2.7. Effects of PDT with PQ on the Ultrastructure and Cell Membrane Integrity

As it was expected that the PQ photolytic products would target cellular structures, it was sought to determine the effects of the resultant reactive oxygen species on the cells' ultrastructure and membrane integrity. A scanning electron microscope (SEM) was used to study the cells' ultrastructure. The SEM protocol was based on the method detailed by Swart and co-workers [35]. In brief, after treatment, cells of the same experimental condition were aspirated and pooled together into 1.5 mL plastic tubes. The plastic tubes were centrifuged for 5 min at 1000× g at 30 °C to pellet the cells. The pelleted cells were then fixed with 1 mL of 3% phosphate-buffered glutaraldehyde for 3 h and washed afterwards with the same buffer. The cells were fixed a second time with 1% sodium buffered osmium tetroxide glutaraldehyde for 1.5 h. Thereafter, graded acetone series of 30, 50, 70, 95 and 100% were used to dehydrate the fixed cells. Following this, cells were critical-point dried, mounted on stubs and coating with gold. The samples were viewed with scanning electron microscopy. A number of images were taken from different positions on the stub. Furthermore, 100 randomly selected cells were considered, and their cell diameters were measured.

Two assays were also performed, viz. a propidium iodide (PI) assay and a Toxilight assay, to assess the impact of PDT on membrane integrity. The PI stain is excluded by a healthy cell with an intact membrane [36], while Toxilight measures the amount of adenylate kinase (AK), an intracellular enzyme that is only secreted into the cultivation media of dead cells once they have lost selective permeability. Once more, the contents of the wells were aspirated and dispensed to corresponding wells in either black (PI) or white (AK) microtiter plates. For the PI exclusion assay, 1 µL of PI stain (10 µg/mL) was added to the wells to react with the cells. The plate was incubated in the dark for 1 h at room temperature and the induced fluorescence was measured at an excitation of 485 nm and emission of 538 nm with a fluorescence plate reader. The reader converts logarithmic signals to relative fluorescence units. For the AK assay, 100 µL of Toxilight reagent was added to the wells to react with the supernatant, and the plate was incubated at room temperature for 10 min in the dark. The induced luminescence was measured after the incubation period with the Fluoroskan Ascent FL microplate reader. The reader converts logarithmic signals to relative luminescence units.

2.8. Effects of PDT with PQ on the Phagocytic Efficiency of Murine Macrophages

We explored the influence of PDT with PQ on the phagocytic capability of macrophages against cryptococcal cells. Here, a number of co-cultured (1 (macrophage): 1 (cryptococcal cell)) experimental conditions were set up at room temperature inside microtiter plates: (1) co-cultured cells with 0 µM of PQ and exposed to DL for 2 min (i.e., non-Rx co-cultured cells); (2) co-cultured cells with 6 µM of PQ and exposed to DL for 2 min (i.e., drug effect); (3) co-cultured cells with 15 µM of PQ and exposed to DL for 2 min (i.e., drug effect); (4) co-cultured cells with 30 µM of PQ and exposed to DL for 2 min (i.e., drug effect); (5) co-cultured cells with 0 µM of PQ and exposed to UVL for 2 min (i.e., UV effect);

(6) co-cultured cells with 6 μM of PQ and exposed to UVL for 2 min (i.e., PDT effect); (7) co-cultured cells with 15 μM of PQ and exposed to UVL for 2 min (i.e., PDT effect), and (8) co-cultured cells with 30 μM of PQ and exposed to UVL for 2 min (i.e., PDT effect). The cells were first allowed to react to PQ for 30 min (in the dark) prior to exposure to UVL (where appropriate).

Following the handling of co-cultured cells as indicated above, the plate was incubated at 37 °C in 5% CO₂ for 18 h. After the incubation period, the supernatant was aspirated and replaced with 200 μL of phosphate-buffered solution (PBS) to wash out the non-internalized cryptococcal cells. The macrophages with internalized cryptococcal cells were harvested by transferring to 1.5 mL plastic tubes. Macrophages were then lysed using 300 μL of 0.1% Triton X-100. At this concentration, Triton X-100 has been reported not to have any effect on the viability of fungi but can lyse macrophage cells [37,38]. A 10 times serial dilution using distilled water was carried out on cryptococcal cells, and 50 μL of the dilution was plated out on YM agar plates. The plates were incubated for 48 h at 30 °C, and colony-forming units (CFUs) were counted.

2.9. Effects of PDT with PQ on the Metabolic Activity of Murine Macrophages

The effect of PDT using PQ on the metabolic activity of murine macrophages was also investigated. The macrophages that were grouped to yield the following experimental conditions at room temperature: (1) macrophages with 0 μM of PQ and exposed to DL for 8 min (i.e., non-Rx macrophages); (2) macrophages with 6 μM of PQ (0.2 \times the MIC) and exposed to DL for 8 min (i.e., drug effect); (3) macrophages with 60 μM of PQ (2 \times the MIC) and exposed to DL for 8 min (i.e., drug effect); (4) macrophages with 600 μM of PQ (20 \times the MIC) and exposed to DL for 8 min (i.e., drug effect); (5) macrophages with 0 μM of PQ and exposed to UVL for 8 min (i.e., UV effect); (6) macrophages with 6 μM of PQ (0.2 \times the MIC) and exposed to UVL for 8 min (i.e., PDT effect); (7) macrophages with 60 μM of PQ (2 \times the MIC) and exposed to UVL for 8 min (i.e., PDT effect), and (8) macrophages with 600 μM of PQ (20 \times the MIC) and exposed to UVL for 2 min (i.e., PDT effect). The macrophages were first allowed to react to PQ for 30 min (in the dark) prior to exposure to UVL (where appropriate).

Following the handling of macrophages as indicated above, they were reacted with XTT and menadione before incubating for 3 h at 37 °C in 5% CO₂. After 3 h, the absorbance of the wells was measured at 492 nm to estimate the metabolic activity of macrophages.

2.10. Statistical Analyses

For each study, three independent experiments were performed. No technical repeats were included for each independent experiment. GraphPad Prism 8.3.1 was used to calculate mean values and the standard deviation of the means. The same program was used to perform the multiple comparison test using Tukey as an option. For proper interpretation of the data, box plots were used as recommended by Weissgerber et al. [39].

3. Results

3.1. Cryptococcal Cells Were Susceptible to the Photodynamic Action of PQ

The response of *C. neoformans* H99 to PDT using PQ is summarized in Figure 1. There was no significant difference ($p \geq 0.5$) in the absorbance readings obtained for the non-treated cells (0 μM and no UVL) when compared to cells treated with PQ alone at 6, 30, or 60 μM . This suggested there was no drug effect. However, there was a UV effect. Despite the noted UV effect, the implementation of PDT (by exposing PQ to UV) resulted in a significant combinatorial effect when compared to non-treated cells ($p \leq 0.01$), drug effect ($p \leq 0.05$), and UV effect ($p \leq 0.05$). PQ at 30 μM was sufficient to inhibit the metabolic activity of the test population of cells by more than 50% when compared to the other two PQ concentrations. Thus, PQ at 30 μM was defined as the MIC in the current study. This concentration was used henceforth as the MIC.

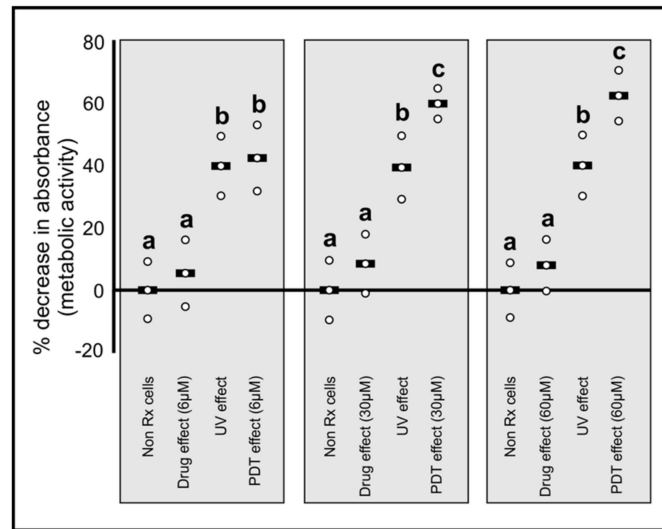


Figure 1. Effect of PDT with PQ on the metabolic activity of *C. neoformans* H99. The decrease in absorbance is against the maximum absorption value of the non-Rx control. A p value of less than or equal to 0.05 was considered significant. A box plot that has a different alphabet to the other box plot implies there is a significant difference ($p < 0.05$) while those with the same alphabet are not significantly different ($p > 0.05$). Black bars = medians; circles = the distribution of the data points.

3.2. PDT with PQ Induces Accumulation of ROS

The ROS data are summarized in Figure 2. The data for non-treated cells were comparable, i.e., no significant difference ($p \geq 0.4$), to that of the drug-alone test. The tested cell population experienced a UV effect. When PDT was implemented, there was a significant accumulation ($p \leq 0.01$) of ROS when the PDT data were compared to that of non-treated cells as well as cells exposed to UVL-alone ($p \leq 0.04$). The accumulation of ROS suggests a type I reaction. This assertion is supported by literature that further documents that the PQ decomposes photochemically by oxygen-dependent reaction mechanisms, wherein free radicals ($\text{OH}\cdot$ and $\text{O}_2\cdot^-$) are formed in the photochemical reactions [40].

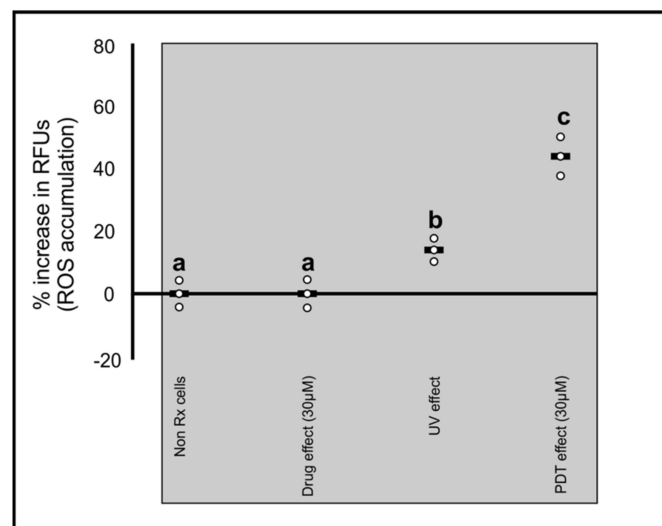


Figure 2. Effect of PDT with PQ on the production of ROS in *C. neoformans* H99. The increase in RFUs is against the maximum fluorescence value of the non-Rx control. A p value of less than or equal to 0.05 was considered significant. A box plot that has a different alphabet to the other box plot implies there is a significant difference ($p < 0.05$) while those with the same alphabet are not significantly different ($p > 0.05$). Black bars = medians; circles = the distribution of the data points.

3.3. The Photolytic Products of PQ Alter the Cryptococcal Ultrastructure and Compromise Cell Membranes

The SEM images that allow for the comparison of the cryptococcal ultrastructure across the different experimental conditions are collated in Figure 3. The outer structure of the non-treated cells (with neither PQ nor UVL) appeared to have rough surfaces covered with an extracellular matrix. The cells were determined to have an average cell diameter ($3.6 \mu\text{m} (+/- 0.1)$). Cells exposed to the drug alone (PQ at $30 \mu\text{M}$) seemed to have a slight to no reduction in the extracellular matrix; moreover, there was no significant reduction ($p \geq 0.05$) in their cell diameter ($3.5 \mu\text{m} (+/- 0.3)$) when compared to non-treated cells. However, cells exposed to UVL seemed to have lost the extracellular matrix and were significantly ($p \leq 0.05$) smaller ($2.9 \mu\text{m} (+/- 0.3)$) when compared to non-treated cells. Cells exposed to PDT also lost the extracellular matrix and were significantly ($p \leq 0.05$) smaller ($2.5 \mu\text{m} (+/- 0.3)$) when compared to non-treated cells.

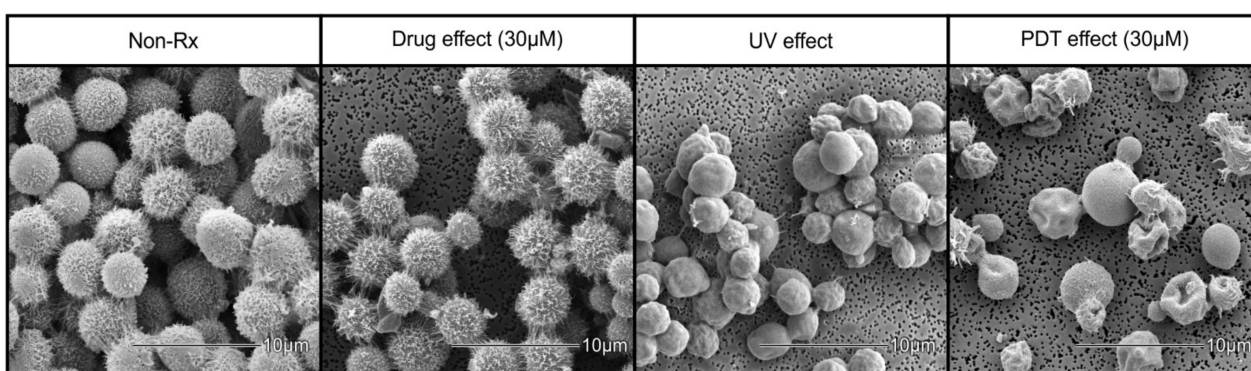


Figure 3. SEM images showing the morphological differences of cryptococcal cells' ultrastructure after being handled in designed experimental groups. The images were taken after studying *C. neoformans* H99 cells.

To further assess the integrity of the cell wall following treatment, the accumulation of PI inside the cells (Figure 4), as well as the release of AK enzyme into the cultivation media (Figure 5), were considered.

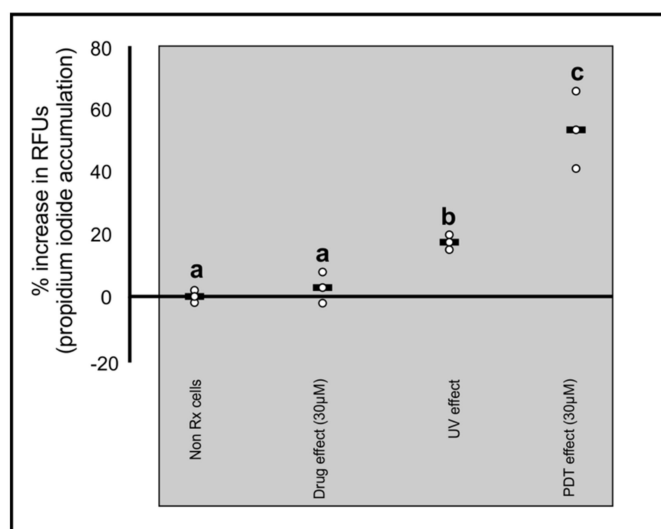


Figure 4. Effect of PDT with PQ on membrane selective permeability in *C. neoformans* H99. Accumulation of propidium iodide was used as an indicator for loss of membrane integrity. The increase in RFUs is against the maximum fluorescence value of the non-Rx control. A p value of less than or equal to 0.05 was considered significant. A box plot that has a different alphabet to the other box plot implies there is a significant difference ($p < 0.05$) while those with the same alphabet are not significantly different ($p > 0.05$). Black bars = medians; circles = the distribution of the data points.

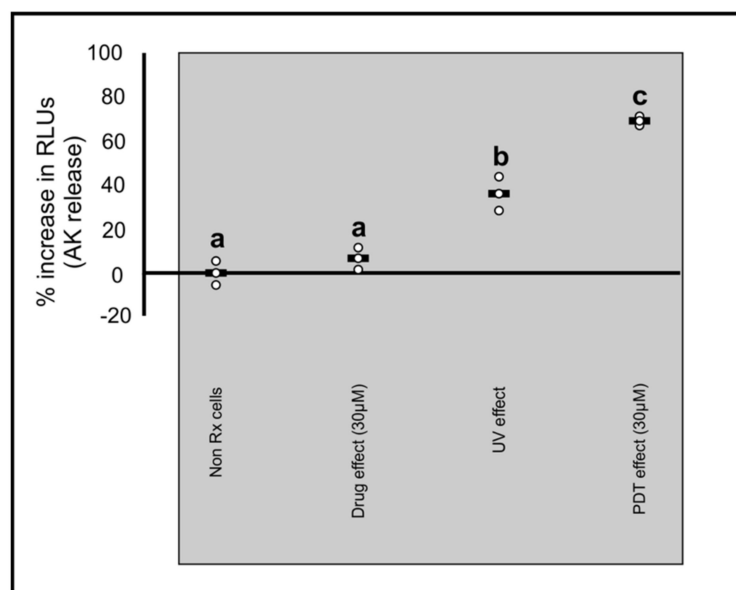


Figure 5. Effect of PDT with PQ on membrane selective permeability in *C. neoformans* H99. Accumulation of adenylate kinase was used as an indicator for loss of membrane integrity. The increase in RLUs is against the maximum luminescence value of the non-Rx control. A p value of less than or equal to 0.05 was considered significant. A p value of less than or equal to 0.05 was considered significant. A box plot that has a different alphabet to the other box plot implies there is a significant difference ($p < 0.05$) while those with the same alphabet are not significantly different ($p > 0.05$). Black bars = medians; circles = the distribution of the data points.

For PI, the data for the non-treated cell was comparable, i.e., no significant difference ($p \geq 0.1$), to that of the drug-alone test. However, the exposure of cells to UVL for 2 min led to a UV effect ($p \leq 0.05$). Despite this UV effect, when combined (30 μ M of PQ and 2 min UVL), there was a significant accumulation of PI inside the cells when compared to non-treated cells ($p \leq 0.03$) and cells exposed to UVL-alone ($p \leq 0.05$). For Toxilight, the data for the non-treated cells was comparable, i.e., no significant difference ($p \geq 0.2$), to that of the drug-alone test. However, the exposure of cells to UVL for 2 min led to a UVL effect ($p \leq 0.05$). Despite this UVL effect, when PDT was effected, there was a significant accumulation ($p \leq 0.01$) of AK in the cultivation media when compared to non-treated cells ($p \leq 0.05$) and cells exposed to UVL-alone ($p \leq 0.05$).

3.4. PDT Improves the Phagocytic Efficiency of Macrophages

Figure 6 represents the CFU counts that were obtained for all the experimental conditions. Co-cultured cells treated with PQ (6, 15, or 30 μ M) did not show any significant decrease ($p \geq 0.3$) in cryptococcal CFU counts compared to the non-treated co-cultured cryptococcal cells. There was also a decrease in the cryptococcal CFU counts of co-cultured cells exposed to UV only; however, it was not significant ($p \geq 0.4$) when compared to the co-cultured cells without any treatment. Exposure of co-cultured cells to PDT with PQ (6 or 15 μ M PQ) did not result in any significant ($p \geq 0.09$) decrease in cryptococcal CFU counts compared to non-treated co-cultured cells. Importantly, a significant decrease ($p < 0.05$) in cryptococcal CFU counts was obtained with the co-cultures that were subjected to the effect of UVL and 30 μ M PQ (MIC that was defined for cryptococcal cells).

3.5. PDT Does Not Negatively Affect the Macrophages

Figure 7 summarizes the response of macrophages to the effect of PDT. There was no notable difference ($p \geq 0.6$) in the absorbance readings obtained for the macrophages that were non-treated (0 μ M, no UVL and in 8 min of DL) when compared to macrophages that were exposed to PQ alone (6, 60, or 600 μ M), UVL-alone (8 min) or PDT (6 μ M and UVL for 8 min, 60 μ M and UVL for 8 min, or 600 μ M and UVL for 8 min). These results

speak to the suitability of applying PDT (even at a higher drug concentration and a longer exposure time) to these immune cells, which are often manipulated by cryptococcal cells during dissemination.

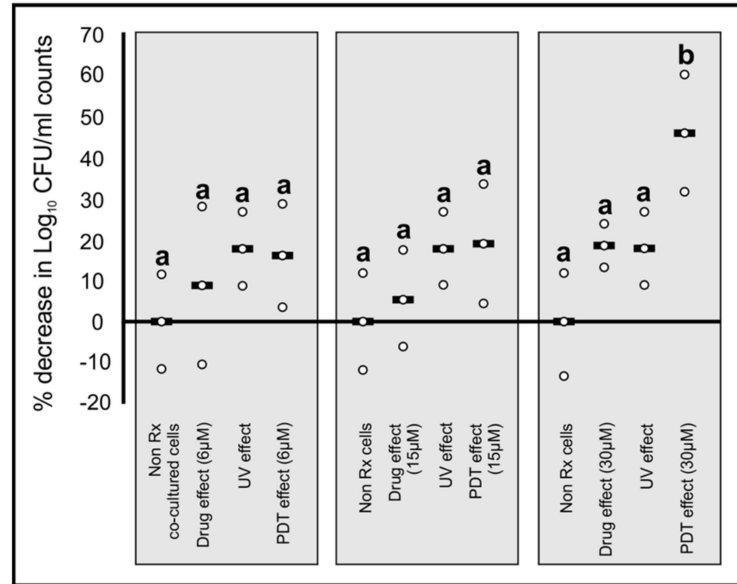


Figure 6. Effect of PDT with PQ on macrophage phagocytic efficiency. A *p* value of less than or equal to 0.05 was considered significant. A box plot that has a different alphabet to the other box plot implies there is a significant difference ($p < 0.05$) while those with the same alphabet are not significantly different ($p > 0.05$). Black bars = medians; circles = the distribution of the data points.

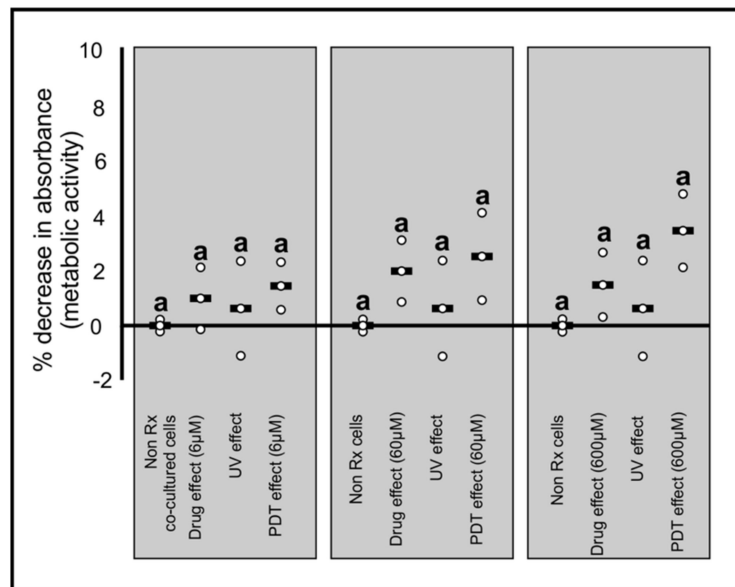


Figure 7. Effect of PDT with PQ on the metabolic activity of macrophages. The decrease in absorbance is against the maximum absorbance value of the non-Rx control. A *p* value of less than or equal to 0.05 was considered significant. A box plot that has a different alphabet to the other box plot implies there is a significant difference ($p < 0.05$) while those with the same alphabet are not significantly different ($p > 0.05$). Black bars = medians; circles = the distribution of the data points.

4. Discussion

Fungal infections may manifest life-threatening diseases, and cryptococcal infections are particularly dangerous to people living with HIV/AIDS. To compound this, short-

comings associated with the current antifungal regimen contribute, in part, to the high cryptococcal mortality rate. This has necessitated the need to consider repurposing PQ as a photosensitizer to inactivate cryptococcal cells. This drug has previously been successfully used outside its prescribed scope in treating *Pneumocystis pneumonia* [31,32].

The current study provides evidence that exposing PQ to UVL was sufficient to sensitize this drug to display an anti-cryptococcal quality. More importantly, it is theorized that these resultant radicals from the photolysis of this compound may have led to cells losing their cell wall integrity and selective permeability. This, in turn, induced cell death. These results support the findings in literature wherein the susceptibility of *C. neoformans* and *Candida albicans* to PDT directly correlates with cell membrane permeability function [19,41]. To illustrate this point, Fuchs et al. demonstrated that the use of polycationic conjugate of polyethyleneimine and photosensitizer chlorin(e6) compromised the integrity of cell walls of *C. neoformans* following PDT [19].

Numerous limitations faced by this type of therapy still need to be overcome for it to be fully appreciated as a therapy for infectious diseases. The crucial issues to address will be modes of delivery of both the light and the photosensitizer to sites of infection. The current knowledge on PDT delivery for infection is limited to the parts of the body that light can reach quite easily, such as skin and body cavities [20]. More to the point, antimicrobial PDT is better applied exclusively to localized diseases, in contrast to systemic infections such as cryptococcal pneumonia, cryptococcal meningitis, and sepsis, among others [19,42]. Importantly, it is necessary to determine the appropriate illumination devices with well-defined parameters and accurate dosimetry [42].

5. Conclusions

The current study has given insight into the potential of PQ as a photosensitizer when used in in vitro studies. However, further in vivo studies should be carried out to validate the obtained results wherein several aspects of photosensitizers need to be well defined in a clinical setting. These include the dose to be delivered and patient acceptability [43]. Moreover, care should be taken to prevent continuous photoreaction by keeping patients away from sources of UVC, as this radiation is damaging. To remedy this, treatment could be administered in the presence of a molecule that could modify how skin epithelial cells receive UV radiation [33]. Fortunately, UVC radiation from the sun is filtered by the atmosphere and, therefore, does not reach the earth's surface.

Author Contributions: Conceptualization, O.M.S.; methodology, U.L.M., A.O.O., O.S.F. and O.M.S.; formal analysis, U.L.M.; investigation, U.L.M. and O.M.S.; resources, O.M.S.; writing—original draft preparation, U.L.M.; writing—review and editing, U.L.M., A.O.O., O.S.F., J.A., C.H.P. and O.M.S.; supervision, J.A., C.H.P. and O.M.S.; project administration, O.M.S.; funding acquisition, O.M.S. All authors have read and agreed to the published version of the manuscript.

Funding: This research was funded by the NATIONAL RESEARCH FOUNDATION OF SOUTH AFRICA, grant number UID 114321 and the University of the Free State.

Data Availability Statement: The data presented in this study are available in the article.

Acknowledgments: Parts of this manuscript are contained in the PhD thesis of U.L.M. The authors are grateful for the services and assistance offered by the following colleagues: PWJ van Wyk and H Globler, for SEM work.

Conflicts of Interest: The authors declare no conflict of interest. The funders had no role in the design of the study; in the collection, analyses, or interpretation of data; in the writing of the manuscript, or in the decision to publish the results.

References

1. Prescott, S.L.; Larcombe, D.L.; Logan, A.C.; West, C.; Burks, W.; Caraballo, L.; Levin, M.; Etten, E.V.; Horwitz, P.; Kozyrskyj, A.; et al. The Skin Microbiome: Impact of Modern Environments on Skin Ecology, Barrier Integrity and Systemic Immune Programming. *World Allergy Organ. J.* **2017**, *10*, 29. [[CrossRef](#)]

2. Lehtimäki, J.; Karkman, A.; Laatikainen, T.; Paalanen, L.; Von Hertzen, L.; Haahtela, T.; Hanski, I.; Ruokolainen, L. Patterns in the Skin Microbiota Differ in Children and Teenagers Between Rural and Urban Environments. *Sci. Rep.* **2017**, *7*, 45651. [[CrossRef](#)]
3. Nestle, F.O.; Di Meglio, P.; Qin, J.Z.; Nickoloff, B.J. Skin Immune Sentinels in Health and Disease. *Nat. Rev. Immunol.* **2009**, *9*, 679–691. [[CrossRef](#)]
4. Neuville, S.; Dromer, F.; Morin, O.; Dupont, B.; Ronin, O.; Lortholary, O.; French Cryptococcosis Study Group. Primary Cutaneous Cryptococcosis: A Distinct Clinical Entity. *Clin. Infect. Dis.* **2003**, *36*, 337–347. [[CrossRef](#)]
5. Chakradeo, K.; Paul Chia, Y.Y.; Liu, C.; Mudge, D.W.; De Silva, J. Disseminated Cryptococcosis Presenting Initially as Lower Limb Cellulitis in a Renal Transplant Recipient—A Case Report. *BMC Nephrol.* **2018**, *19*, 18. [[CrossRef](#)] [[PubMed](#)]
6. Casadevall, A. Cryptococci at the Brain Gate: Break and Enter or Use a Trojan Horse? *J. Clin. Investig.* **2010**, *120*, 1389–1392. [[CrossRef](#)]
7. Voelz, K.; May, R.C. Cryptococcal Interactions with the Host Immune System. *Eukaryot. Cell* **2010**, *9*, 835–846. [[CrossRef](#)] [[PubMed](#)]
8. Rajasingham, R.; Smith, R.M.; Park, B.J.; Jarvis, J.N.; Govender, N.P.; Chiller, T.M.; Denning, D.W.; Loyse, A.; Boulware, D.R. Global Burden of Disease of HIV-Associated Cryptococcal Meningitis: An Updated Analysis. *Lancet Infect. Dis.* **2017**, *17*, 873–881. [[CrossRef](#)]
9. Cowen, L.E. The Evolution of Fungal Drug Resistance: Modulating the Trajectory from Genotype to Phenotype. *Nat. Rev. Microbiol.* **2008**, *6*, 187–198. [[CrossRef](#)] [[PubMed](#)]
10. Govender, N.P.; Roy, M.; Mendes, J.F.; Zulu, T.G.; Chiller, T.M.; Karstaedt, A.S. Evaluation of Screening and Treatment of Cryptococcal Antigenaemia among HIV-Infected Persons in Soweto, South Africa. *HIV Med.* **2015**, *16*, 468–476. [[CrossRef](#)] [[PubMed](#)]
11. Ghannoum, M.A.; Rice, L.B. Antifungal Agents: Mode of Action, Mechanisms of Resistance and Correlation of These Mechanisms with Bacterial Resistance. *Clin. Microbiol. Rev.* **1999**, *12*, 501–517. [[CrossRef](#)]
12. Truong, M.; Monahan, L.G.; Carter, D.A.; Charles, I.G. Repurposing Drugs to Fast-Track Therapeutic Agents for the Treatment of Cryptococcosis. *PeerJ* **2018**, *6*, e4761. [[CrossRef](#)]
13. Saag, M.S.; Graybill, R.J.; Larsen, R.A.; Pappas, P.G.; Perfect, J.R.; Powderly, W.G.; Sobel, J.D.; Dismukes, W.E. Practice Guidelines for the Management of Cryptococcal Disease. *Clin. Infect. Dis.* **2000**, *30*, 710–718. [[CrossRef](#)] [[PubMed](#)]
14. Ho, J.; Fowler, P.; Heidari, A.; Johnson, R.H. Intrathecal Amphotericin B: A 60-Year Experience in Treating Coccidioidal Meningitis. *Clin. Infect. Dis.* **2016**, *64*, 519–524. [[CrossRef](#)]
15. Cuddihy, G.; Wasan, E.K.; Di, Y.; Wasan, K.M. The Development of Oral Amphotericin B to Treat Systemic Fungal and Parasitic Infections: Has the Myth Been Finally Realised? *Pharmaceutics* **2019**, *11*, 99. [[CrossRef](#)] [[PubMed](#)]
16. Bicanic, T.; Harrison, T.; Niepieklo, A.; Dyakopu, N.; Meintjes, G. Symptomatic Relapse of HIV-Associated Cryptococcal Meningitis after Initial Fluconazole Monotherapy: The Role of Fluconazole Resistance and Immune Reconstitution. *Clin. Infect. Dis.* **2006**, *43*, 1069–1073. [[CrossRef](#)]
17. Jarvis, J.N.; Bicanic, T.; Loyse, A.; Namarika, D.; Jackson, A.; Nussbaum, J.C.; Longley, N.; Muzoora, C.; Phulusa, J.; Taseera, K.; et al. Determinants of Mortality in a Combined Cohort of 501 Patients With HIV-Associated Cryptococcal Meningitis: Implications for Improving Outcomes. *Clin. Infect. Dis.* **2014**, *58*, 736–745. [[CrossRef](#)]
18. Smith, K.D.; Achan, B.; Hullsiek, K.H.; McDonald, T.R.; Okagaki, L.H.; Alhadab, A.A.; Akampurira, A.; Rhein, J.R.; Meya, D.B.; Boulware, D.R.; et al. Increased Antifungal Drug Resistance in Clinical Isolates of *Cryptococcus neoformans* in Uganda. *Antimicrob. Agents Chemother.* **2015**, *59*, 7197–7204. [[CrossRef](#)]
19. Fuchs, B.B.; Tegos, G.P.; Hamblin, M.R.; Mylonakis, E. Susceptibility of *Cryptococcus neoformans* to Photodynamic Inactivation Is Associated with Cell Wall Integrity. *Antimicrob. Agents Chemother.* **2007**, *51*, 2929–2936. [[CrossRef](#)]
20. Dai, T.; Fuchs, B.B.; Coleman, J.J.; Prates, R.A.; Astrakas, C.; St Denis, T.G.; Ribeiro, M.S.; Mylonakis, E.; Hamblin, M.R.; Tegos, G.P. Concepts and Principles of Photodynamic Therapy as an Alternative Antifungal Discovery Platform. *Front. Microbiol.* **2012**, *3*, 120. [[CrossRef](#)] [[PubMed](#)]
21. Prates, R.A.; Fuchs, B.B.; Mizuno, K.; Naqvi, Q.; Kato, I.T.; Ribeiro, M.S.; Mylonakis, E.; Tegos, G.P.; Hamblin, M.R. Effect of Virulence Factors on the Photodynamic Inactivation of *Cryptococcus neoformans*. *PLoS ONE* **2013**, *8*, e54387. [[CrossRef](#)] [[PubMed](#)]
22. Baltazar, L.M.; Ray, A.; Santos, D.A.; Cisalpino, P.S.; Friedman, A.J.; Nosanchuk, J.D. Antimicrobial Photodynamic Therapy: An Effective Alternative Approach to Control Fungal Infections. *Front. Microbiol.* **2015**, *6*, 202. [[CrossRef](#)] [[PubMed](#)]
23. Saini, R.; Lee, N.V.; Liu, K.Y.P.; Poh, C.F. Prospects in the Application of Photodynamic Therapy in Oral Cancer and Premalignant Lesions. *Cancers* **2016**, *8*, 83. [[CrossRef](#)] [[PubMed](#)]
24. Josefsen, L.B.; Boyle, R.W. Photodynamic Therapy and the Development of Metal-Based Photosensitisers. *Met. Based Drugs* **2008**, *2008*, 276109. [[CrossRef](#)]
25. Hamblin, M.R.; Hasan, T. Photodynamic Therapy: A New Antimicrobial Approach to Infectious Disease? *Photochem. Photobiol. Sci.* **2004**, *3*, 436–450. [[CrossRef](#)]
26. Wainwright, M.; Crossley, K.B. Methylene Blue—A therapeutic dye for all seasons? *J. Chemother.* **2002**, *14*, 431–443. [[CrossRef](#)]
27. Slater, A.F.G. Chloroquine: Mechanism of Drug Action and Resistance in *Plasmodium falciparum*. *Pharmacol. Ther.* **1993**, *57*, 203–235. [[CrossRef](#)]
28. Foley, M.; Tilley, L. Quinoline Antimalarials: Mechanisms of Action and Resistance and Prospects for New Agents. *Pharmacol. Ther.* **1998**, *79*, 55–87. [[CrossRef](#)]

29. Percário, S.; Moreira, D.R.; Gomes, B.A.Q.; Ferreira, M.E.S.; Gonçalves, A.C.M.; Laurindo, P.S.O.C.; Vilhena, T.C.; Dolabela, M.F.; Green, M.D. Oxidative Stress in Malaria. *Int. J. Mol. Sci.* **2012**, *13*, 16346–16372. [[CrossRef](#)] [[PubMed](#)]
30. Ha, Y.R.; Hwang, B.G.; Hong, Y.; Yang, H.W.; Lee, S.J. Effect of Farnesyltransferase Inhibitor R115777 on Mitochondria of *Plasmodium falciparum*. *Korean J. Parasitol.* **2015**, *53*, 421–430. [[CrossRef](#)] [[PubMed](#)]
31. Toma, E. Clindamycin/Primaquine for Treatment of *Pneumocystis carinii* Pneumonia in AIDS. *Eur. J. Clin. Microbiol. Infect. Dis.* **1991**, *10*, 210–213. [[CrossRef](#)]
32. Noskin, G.A.; Murphy, R.L.; Black, J.R.; Phair, J.P. Salvage Therapy with Clindamycin/Primaquine for *Pneumocystis carinii* Pneumonia. *Clin. Infect. Dis.* **1992**, *14*, 183–188. [[CrossRef](#)] [[PubMed](#)]
33. Ogundeji, A.O.; Mjokane, N.; Folorunso, O.S.; Pohl, C.H.; Nyaga, M.M.; Sebolai, O.M. The Repurposing of Acetylsalicylic Acid as a Photosensitizer to Inactivate the Growth of Cryptococcal Cells. *Pharmaceuticals* **2021**, *14*, 404. [[CrossRef](#)]
34. Harrington, B.; Valigosky, M. Monitoring Ultraviolet Lamps in Biological Safety Cabinets with Cultures of Standard Bacterial Strains on TSA Blood Agar. *Lab. Med.* **2007**, *38*, 165–168. [[CrossRef](#)]
35. Swart, C.W.; Swart, H.C.; Coetsee, E.; Pohl, C.H.; van Wyk, P.W.J.; Kock, J.L.F. 3-D Architecture and Elemental Composition of Fluconazole Treated Yeast Asci. *Sci. Res. Essays* **2010**, *5*, 3411–3417.
36. Hussain, H.; Raj, L.S.; Ahmad, S.; Abd. Razak, M.F.; Wan Mohamud, W.N.; Bakar, J.; Ghazali, H.M. Determination of Cell Viability Using Acridine Orange/Propidium Iodide Dual-Spectrofluorometry Assay. *Cogent Food Agric.* **2019**, *5*, 1582398. [[CrossRef](#)]
37. Levitz, S.M.; Harrison, T.S.; Tabuni, A.; Liu, X. Chloroquine Induces Human Mononuclear Phagocytes to Inhibit and Kill *Cryptococcus neoformans* by a Mechanism Independent of Iron Deprivation. *J. Clin. Investig.* **1997**, *100*, 1640–1646. [[CrossRef](#)]
38. Shen, Q.; Beucler, M.J.; Ray, S.C.; Rappleye, C.A. Macrophage Activation by IFN- γ Triggers Restriction of Phagosomal Copper from Intracellular Pathogens. *PLoS Pathog.* **2018**, *14*, e1007444. [[CrossRef](#)]
39. Weissgerber, T.L.; Milic, N.M.; Winham, S.J.; Garovic, V.D. Beyond Bar and Line Graphs: Time for a New Data Presentation Paradigm. *PLoS Biol.* **2015**, *13*, e1002128. [[CrossRef](#)] [[PubMed](#)]
40. Kristensen, S.; Edge, R.; Tønnesen, H.H.; Bisby, R.H.; Navaratnam, S. Photoreactivity of Biologically Active Compounds. XIX: Excited States and Free Radicals from the Antimalarial Drug Primaquine. *J. Photochem. Photobiol. B.* **2009**, *94*, 147–157. [[CrossRef](#)] [[PubMed](#)]
41. Giroldo, L.M.; Felipe, M.P.; de Oliveira, M.A.; Munin, E.; Alves, L.P.; Costa, M.S. Photodynamic Antimicrobial Chemotherapy (PACT) with Methylene Blue Increases Membrane Permeability in *Candida albicans*. *Lasers Med. Sci.* **2009**, *24*, 109–112. [[CrossRef](#)] [[PubMed](#)]
42. Kharkwal, G.B.; Sharma, S.K.; Huang, Y.Y.; Dai, T.; Hamblin, M.R. Photodynamic Therapy for Infections: Clinical Applications. *Lasers Surg. Med.* **2011**, *43*, 755–767. [[CrossRef](#)] [[PubMed](#)]
43. Kim, M.M.; Darafsheh, A.; Ahmad, M.; Finlay, J.C.; Zhu, T.C. PDT Dose Dosimeter for Pleural Photodynamic Therapy. *Proc. SPIE Int. Soc. Opt. Eng.* **2016**, *9694*, 96940Y. [[CrossRef](#)] [[PubMed](#)]